



Modeling and position control of the inverted pendulum system

Daryoush Vakili* , Sıtkı Öztürk , Caner Özdemir 

Department of Electronics and Telecommunications Engineering, Faculty of Engineering, University of Kocaeli, Izmit, Turkey

*Corresponding author: daryoush.vakili@gmail.com

(Received: April 9, 2024 / Accepted: June 3, 2024)

Abstract

It is difficult to find the unknown/unmeasurable parameters of in system and the control parameters of the system by experimenting on the real system. The aim of this study is to first find the unknown parameters of the system by creating a mathematical model of the system in a simulation environment, and then to obtain the PID control parameters in the simulation environment with the found parameters. Thus, to see the conformity of the control of the real system to the mathematical model and to show that the unknown parameters can be easily found through simulation. In this study, the position control of the inverted pendulum system, which is one of the control system examples, was carried out to maintain balance. For position control, a mathematical model of the system was first created, then a simulation model was created and experiments were conducted. Experiments were then conducted on a real system using the parameters obtained from the system simulation model. In this study, the car to which the pendulum was connected was controlled to maintain the inverted pendulum system in balance. In the system, a servo motor is used to move the car. The balance position is controlled by moving the car along the horizontal axis. An encoder with a full revolution of 4096 pulses was used to obtain the balance position information of the inverted pendulum. The sensitivity of the encoder used is approximately 11.37 pulses per degree. The experimental setup of the system was created by connecting the rod used as an inverted pendulum to the Encoder. The experimental setup was controlled with a program written in PLC (programmable logic controller). The servo motor that moves the car to ensure that the inverted pendulum remains in balance is controlled by the driver. The servo motor driver was driven by a control signal with ± 10 volts sent from the PLC. The servo motor driver is programed to run at ± 1000 rpm in response to this control signal. The unmeasurable parameters of the system were experimentally determined. For this purpose, the parameters in the mathematical model were obtained by swarm optimization (PSO) using the measurement values obtained by operating the experimental setup as a simple pendulum. A simulation model of the system was created using the parameters obtained with PSO and the mathematical model. PID (Proportional Integral Derivative) controller was used in the simulation model. The PID parameters required to control the system were obtained using particle swarm optimization in the simulation model. The PID parameters obtained using PSO were used as the parameters of the PID controller in the real experimental system. It was observed that the results obtained in the simulation system and those obtained in the real system overlapped, and the design of the simulation model in this study was successful.

Keywords: Inverted Pendulum, PID Control, Position Control, PSO, PLC.

Introduction

In this study, balance control of the inverted pendulum system was performed using a simulation model and an experimental set. A PID controller was used as the controller for the systems. Generally, in control applications of the inverted pendulum system, the aim is to keep the inverted pendulum in balance with the movement of the car. In addition, in some applications, keeping the cart at a certain distance is performed as a second control. In this study, it is aimed to remain in the equilibrium position (0 degrees) of the pendulum when the equilibrium position of the pendulum is disrupted by a disturbing effect, without being concerned with the position of the cart. The real system shown in Figure 1 comprises a cart that can move on the horizontal axis and a rod mechanism connected to the cart with an encoder. The movement of the car is achieved by converting the circular motion taken from the servo motor into planar motion using a toothed chain belt. By operating the servo motor driver in ± 10 volt analog input mode, forward and reverse movement of the servo motor can be achieved. This analog input signal is the controller signal used to control the inverted pendulum. An encoder was used in the system to obtain the position information of the

inverted pendulum. The full revolution of the encoder is 4096 pulses, and this value corresponds to 360° . A PLC was used as the controller in the system. To find the parameters that cannot be measured in the system, free oscillation information of the system was taken from the real system. On the mathematical model of the system, the unmeasurable parameters of the system were determined using the Particle Swarm Optimization (PSO) algorithm with the free oscillation data from the system to determine the unmeasurable parameters (friction and moment of inertia). PID control was used in the simulation model of the system with the friction and moment of inertia obtained from the PSO algorithm. The parameters of the PID controller were also obtained using the PSO algorithm. matching control results were obtained by running both the simulation and the real system with these values.

There are two balance points in inverted pendulum systems. The first equilibrium point is the position where the pendulum is stable at the bottom, which is the simple pendulum position. The second equilibrium point is the unstable position, where the pendulum is up vertically in the inverted pendulum position at an angle of 180° relative to the simple pendulum.

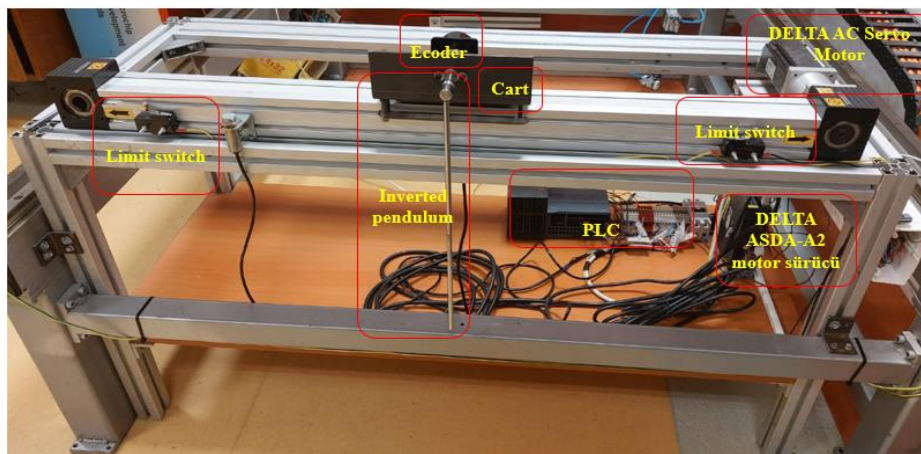


Figure 1. Controlled inverted pendulum system experimental setup

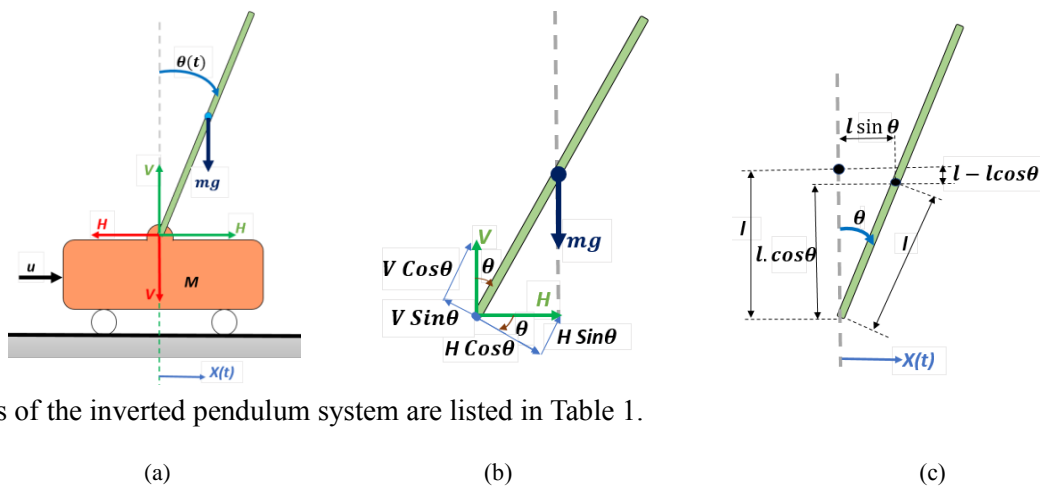
The first research on pendulum oscillations was conducted by Ibn Yunus in the 10th century [1-2]. Nasir and his colleagues applied PID, a classical control method, and sliding mode control, a modern control method, to a linear carriage inverted pendulum system and compared the success of these two control methods on the balancing problem according to their time characteristics. Based on the simulation results and after assessing the control performance of both methods, they found that the sliding mode control performed better than the PID method [3]. Kizir focused on both the swing-up and balancing problems of the inverted pendulum and applied it to the system in real time using different control methods. He used energy-based and fuzzy logic control methods to raise the pendulum, and in each method, he moved the pendulum for 10 seconds. brought it to the desired vertical position. To balance the pendulum, PID, full state feedback, and fuzzy logic methods were applied to the system. He examined the robustness of each control method and provided both simulation and experimental results [4]. Aström et al. examined amplification strategies based on the energy control method in inverted pendulum systems and explained the results with simulations for different situations [5]. Aracil et al. designed a controller based on the speed guard method for controlling a rotary inverted pendulum or furta pendulum system [6]. In current control studies, computer-based simulation and implementation programs are used to create a mathematical model of the system to be controlled [7-9] and to subject the created model to theoretical fictions. The purpose of automatic control is to provide a stable operating environment by maintaining the control variables of the systems at the desired values. The aim of automation systems is to prevent possible oscillations and maintain system stability by quickly reacting to the effects occurring in the system [10-11]. The PID controller is the most widely used controller type in the industry to ensure the stability of the system [12-16]. In this study, the system will first be controlled through the simulation model, and then the real system will be controlled using the controller designed with simulation.

Mathematical Model of the Inverted Pendulum System

The inverted pendulum system consists of a cart and a rod mounted on the cart, as shown in Figure 2. In the

figure, u is the control force that allows the cart to move horizontally. Because of this movement, the rod (inverted pendulum) on the cart moves, disrupting its equilibrium position. The rod moves in a circular motion, with the center of the circle being the rod and the cart's attachment point.

By controlling the movement of the cart with the force u , it is aimed that the rod stays balanced against disturbance, that is, it remains in an upright position in equilibrium. As seen in Figure 2, in the inverted pendulum system, a cart's weight M consists of a pendulum of size l and weight m . The gravity acting on the inverted pendulum is denoted g . The moment of inertia of the inverted pendulum is denoted by J . Since there is very little friction between the inverted pendulum and the car, it is assumed to be zero. H and V are shown as the horizontal and vertical components of the forces acting on the cart and the inverted pendulum. The



parameters of the inverted pendulum system are listed in Table 1.

Figure 2. Forces acting on the inverted pendulum and the car. (a) Forces acting on the cart and the inverted pendulum. (b) Forces acting on the inverted pendulum. (c) Position of the inverted pendulum as a result of the cart moving forward $x(t)$.

Table 1. Parameters of the inverted pendulum experimental setup

Model Parameters	Symbol	Value	Unit
Cart weight	M	1.9	kg
Pendulum weight	m	0.122	kg
Pendulum length	l	0.39	m
Gravitational acceleration	g	9.80	m/s ²
System impact force	u	-	N
Pendulum angle	θ	-	rad
Horizontal force acting on the pendulum	H	-	N
Vertical force acting on the pendulum	V	-	N
Direction of movement of the car	M	-	m

If an object of weight m moves with acceleration a , the resulting force is generally written as given in Equation 1, using Newton's second law of motion.

$$F = ma$$

Equation 1

In Equation 2, u is written as the force applied to the cart and on its horizontal axis. In Figure 2, when the cart of weight M moves in the x -direction, the horizontal forces that occur in the system are given by Equation 2.

$$M \frac{d^2x}{dt^2} = u - H$$

Equation 2

In Figure 2b, the new horizontal position of the pendulum because of the x movement of the cart will be $(x + l \sin\theta)$. Therefore, the forces of the inverted pendulum with weight m on the horizontal axis are written as in Equation 3 using Newton's second law of motion.

$$m \frac{d^2}{dt^2} (x + l \sin\theta) = H$$

Equation 3

In Figure 2b, the new vertical position of the pendulum because of the x movement of the cart will be $(l - l \cos\theta)$. Vertical forces acting on the inverted pendulum system are given by Equation 4.

$$m \frac{d^2}{dt^2} (l - l \cos\theta) + V = mg$$

Equation 4

If Equation 4 is arranged, the result is Equation 5.

$$m \frac{d^2}{dt^2} (-l \cos\theta) + V = mg$$

Equation 5

In Equation 6, the moment of inertia of the inverted pendulum is given in Figure 2 (b). Moment of inertia or the moment of inertia that opposes the rotation of the inverted pendulum,

$$J \frac{d^2\theta}{dt^2} = l \cdot V \sin\theta - l \cdot H \cos\theta$$

Equation 6

For a small value of θ in Equation 6, if $\cos\theta \approx 1$ and $\sin\theta \approx \theta$ are accepted, the linearized inertia equation of the system is given in Equation 7.

$$J \frac{d^2\theta}{dt^2} = V \cdot \theta \cdot l - H \cdot l$$

Equation 7

If the same assumption is made for the small value of θ in Equation 3, the result is given by Equation 8.

$$m \frac{d^2}{dt^2} (x + l \cdot \theta) = H$$

Equation 8

If the same assumption is made for the small value of θ in Equation 5, it becomes Equation 9.

$$m \frac{d^2}{dt^2} (-l) + V = mg$$

$$V = mg$$

Equation 9

If Equations 8 and 9 are replaced in Equation 7, the result is Equation 10.

$$J \frac{d^2\theta}{dt^2} = m g \theta l - m \frac{d^2}{dt^2} (x + l \theta) l$$

$$J \frac{d^2\theta}{dt^2} = m g \theta l - m \frac{d^2}{dt^2} (x l + l^2 \theta)$$

Equation 10

If Equation 10 is written, it regularly becomes Equation 11.

$$(J + ml^2) \frac{d^2\theta}{dt^2} + ml \frac{d^2x}{dt^2} - mgl\theta = 0$$

Equation 11

Equation 10 was obtained as the first linear equation of the inverted pendulum system. If Equation 8 is written in Equation 12.

$$M \frac{d^2x}{dt^2} = u - m \frac{d^2}{dt^2} (x + l \theta)$$

$$(M + m) \frac{d^2x}{dt^2} + ml \frac{d^2\theta}{dt^2} = u$$

Equation 12

Equation 11 is obtained as the second linear equation of the inverted pendulum system. If the transfer function of the inverted pendulum system is adjusted by taking the Laplace transformation of Equation 10, we obtain Equation 13.

$$(J + ml^2)s^2\theta(s) + mls^2X(s) - mgl\theta(s) = 0$$

$$((J + ml^2)s^2 - mgl) \theta(s) + mls^2X(s) = 0$$

$$X(s) = \frac{(mgl - (J + ml^2)s^2)}{mls^2} \theta(s)$$

Equation 13

The transfer function of the angle change of the inverted pendulum in response to the applied force to the system is obtained as in Equation 13 by taking the Laplace transform of Equation 11, substituting X(s) for X(s) in Equation 12, and making adjustments to give Equation 14.

$$(M + m)s^2X(s) + mls^2\theta(s) = U(s)$$

$$(M + m)s^2 \frac{(mgl - (J + ml^2)s^2)}{mls^2} \theta(s) + mls^2\theta(s) = U(s)$$

$$(M + m) \frac{(mgl - (J + ml^2)s^2)}{ml} \theta(s) + mls^2\theta(s) = U(s)$$

$$\frac{m^2l^2s^2 + (M + m)(mgl - (J + ml^2)s^2)}{ml} \theta(s) = U(s)$$

$$\frac{(m^2l^2 - (M + m)(J + ml^2))s^2 + (M + m)mgl}{ml} \theta(s) = U(s)$$

$$\frac{\theta(s)}{U(s)} = \frac{ml}{(m^2l^2 - (M + m)(J + ml^2))s^2 + (M + m)mgl}$$

Equation 14

The transfer function of the system is Equation 14, and the simulation model of the system was prepared from Equations 10 and 11, and the obtained simulation model is shown in Figure 3.

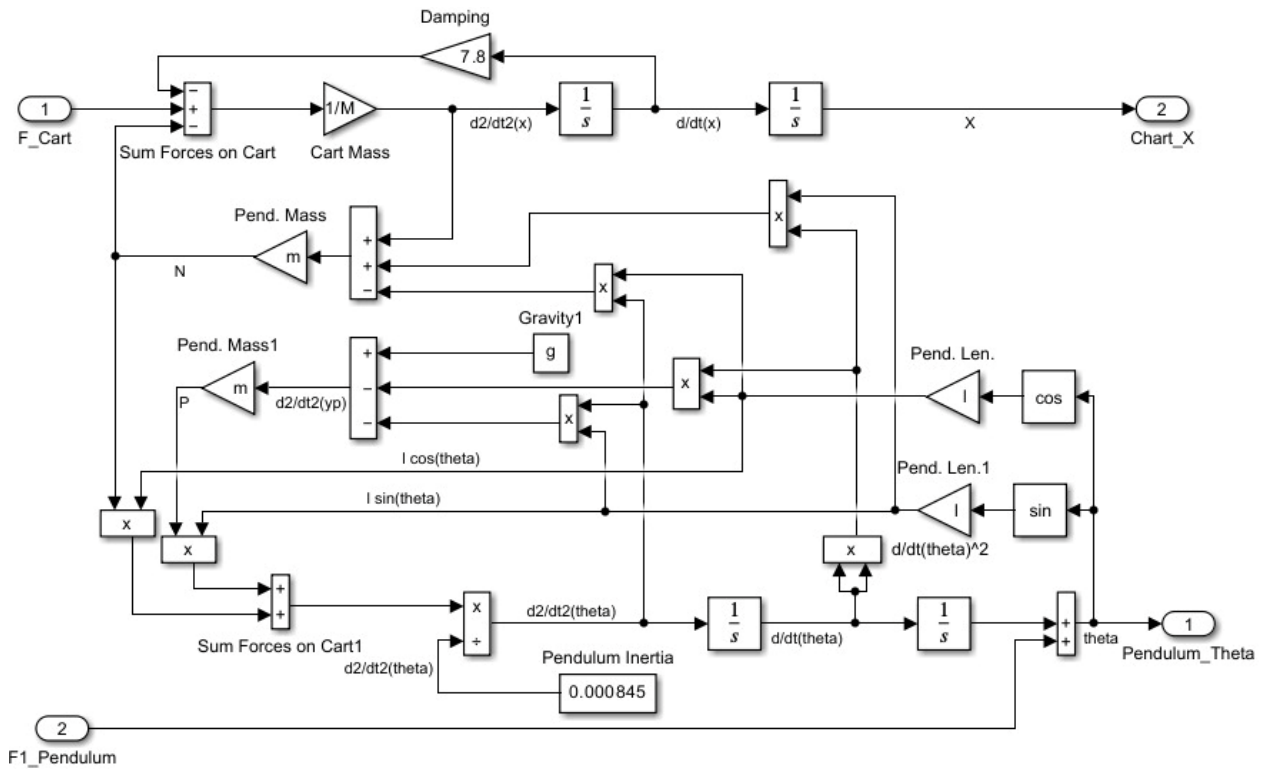


Figure 3. Simulation model of an inverted pendulum

Materials and Methods

Particle Swarm Optimization (PSO)

Optimization algorithms are computational methods developed to find the best possible solution to a specific problem. These algorithms are designed to evaluate different candidate solutions until an optimal solution is found. Issues can have multiple conditions, constraints, and dependencies. Among the optimization algorithms, the PSO algorithm is an optimization method inspired by the behavior of bird flocks or fish schools, hence the name swarm.

PSO was first proposed as a stochastic optimization algorithm by Eberhart and Kennedy in 1995 [21]. The basis of PSO is to simulate the social behavior observed in bird flocks to identify optimal foraging or migration routes. In PSO, the particle distribution represents efficient solutions to the optimization problem. Each particle moves in the search space with the best swarm performance under the influence of its own experience and the particles' common knowledge. Figure 4 shows the movement of the swarm to reach the target/bait in red.

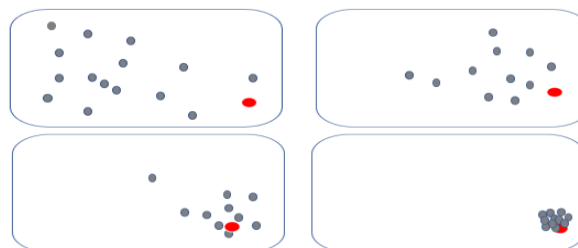


Figure 4. Progress of the swarm toward the target/bait and swarm movement

The PSO algorithm starts by taking a random particle swarm and trying to find the most efficient solution at each renewal. At each refresh (iteration), particle positions are updated on the basis of the two “best values”. The first “best value” is the best solution that the particles have achieved in that iteration. This value is stored

as 'pbest'. The second "best value" is the best solution obtained by all particles in the swarm so far, which is the global best solution, and it is stored with 'gbest'. The swarm particle matrix for 'n' particles consisting of 'm' variables will be as in Equation 15.

$$x = \begin{bmatrix} x_{11} & x_{11} & \dots & \dots & \dots & x_{1m} \\ x_{21} & x_{21} & \dots & \dots & \dots & x_{2m} \\ \dots & \dots & \dots & \dots & \dots & \dots \\ x_{n1} & x_{n1} & \dots & \dots & \dots & x_{nm} \end{bmatrix}_{n \times m}$$

Equation 15

In Equation 15, the i 'th row represents the i 'th particle $x_i = [x_{i1} \ x_{i2} \ \dots \ \dots \ x_{im}]$ is recognized as. The with particle that provided the previous best solution value $pbest_i = [p_{i1} \ p_{i2} \ \dots \ \dots \ p_{im}]$ is taken as. In each iteration, the global best $gbest = [p_1 \ p_2 \ \dots \ \dots \ p_m]$ will be obtained as. The i 'th particle velocity $v_i = [v_{i1} \ v_{i2} \ \dots \ \dots \ v_{im}]$ will be. After finding $pbest$ and $gbest$ values, the particle velocities and new solutions are renewed with Equations 16 and 17.

$$v_i^{k+1} = w \cdot v_i^k + c_1 \cdot rand_1^k \cdot (pbest_i^k - x_i^k) + c_2 \cdot rand_2^k \cdot (gbest^k - x_i^k)$$

Equation 16

$$x_i^{k+1} = x_i^k + v_i^{k+1}$$

Equation 17

In Equation 16, c_1 and c_2 are the learning factors that lead each particle to the best and the best solutions, respectively. c_1 are the constants that enable the particle to move according to its own experience, and c_2 to move according to the experiences of other particles in the swarm. In studies conducted with PSO, researchers stated that taking $c_1 = c_2 = 2$ gave good results. The rand in the equation is uniformly distributed random numbers in the range 0.1. k is the number of renewals. Below is the pseudocode used for the PSO algorithm.

x_{ij} ve v_{ij} create the swarm with random starting values.

Do

```

For  $i = 1$  To  $n$  // Number of particles
  If  $f(x_i) < f(y_i)$  Then  $y_i = x_i$  // Update the local best
   $\hat{y}_i = \min(x_{ij})$  // Update the global best
  For  $j = 1$  To  $m$  // Optimized number of variables
    Equation 16 // Update velocity vector
    Equation 17 // Update the solution vector
  Next  $j$ 
Next  $i$ 

```

Until Continue the maximum number of refreshes and minimum error criteria are met.

In this study, friction and moment of inertia were determined using the simulation model of the system with the PSO algorithm. Similarly, the PSO algorithm was used to determine the PID coefficients for the PID controller design.

Determining the unmeasurable parameters of the system

In this study, the unmeasurable parameters of the system were determined using the PSO algorithm, and the system data given in Figure 5 were obtained by the free oscillation of the inverted pendulum system. To record the free oscillation of the system, the inverted pendulum was let go at 90° and the rod oscillated, while the pendulum came into balance. The oscillation data were measured at a 10-ms sample rate, and the record data shown in Figure 5 were obtained.

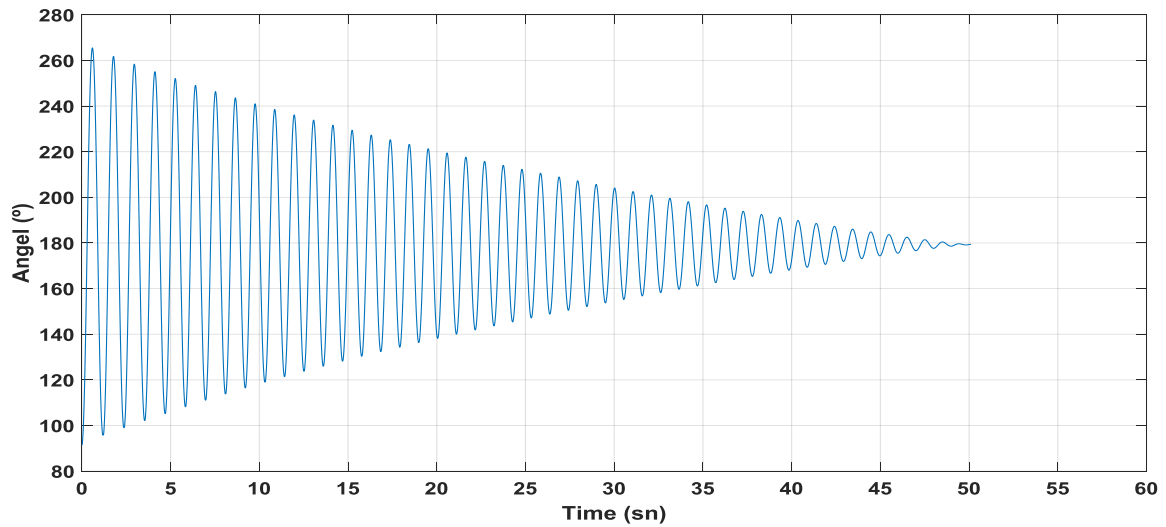


Figure 5. Free swing (free oscillation) behavior of an inverted pendulum released from 90°

The friction and moment of inertia of the system were determined using oscillation data taken from the real system, as shown in Figure 5. In the simulation model of the system, friction and moment of inertia were found using the values that minimized the error between the system simulation output obtained using the PSO algorithm and the data taken from the real system. The friction and moment of inertia parameter values are given in Table 2, and the oscillation obtained when the simulation model of the system is run with the parameters is given in Figure 6.

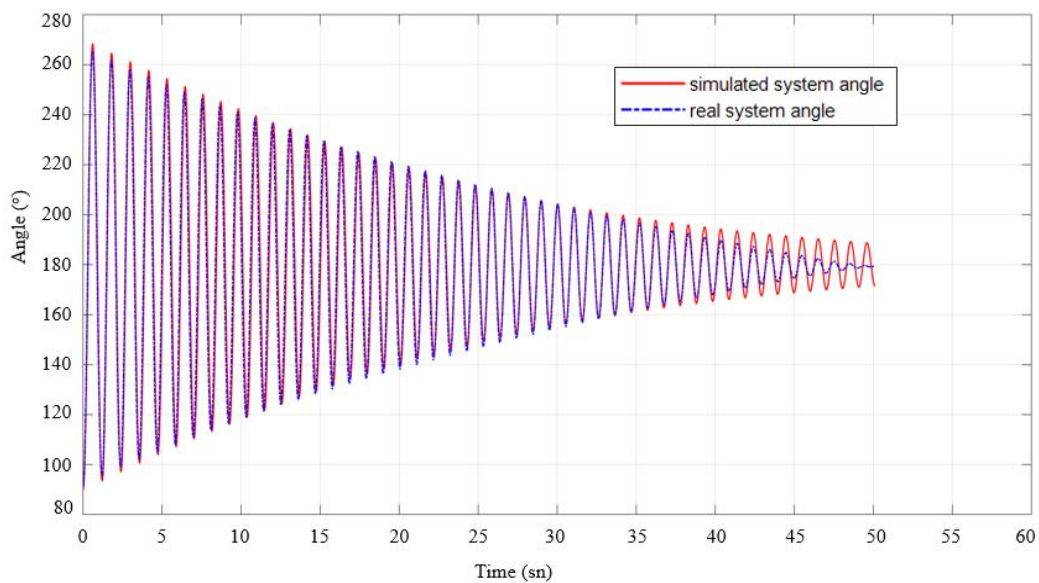


Figure 6. Free oscillation behavior of the real system (blue) and the simulation system (red)

Table 2. Unmeasurable parameters of the system found with PSO from the simulation model

Model Parameters	Symbol	Value	Unit
Friction	b	12	N/m/Sn
Moment of inertia	i	0.000845	Kg m ²

PID Controller

PID (proportional–integral–derivative) controller is one of the most common feedback controllers used in many control processes such as speed, pressure, and temperature control. The PID controller is applied to the system input by generating a control signal to reset the "error" value between the system output value and the desired input value [17]. Although the PID control method is generally used in linear systems, it is also used in many nonlinear systems [18-20]. The mathematical expression of the PID controller is given in Equation 18.

$$u(t) = K_p e(t) + K_i \int_{-\infty}^t e(\tau) d\tau + K_d \frac{d}{dt} e(t)$$

Equation 18

In Equation 18, $u(t)$ produces the control signal produced by the PID and $e(t)$ produces the error signal accordingly. For the PID controller to follow the desired reference value of the system output under the desired conditions, the K_p , K_d and K_i parameters must be appropriately determined. Figure 7 shows the discrete-time PID simulation block created in the simulation model.

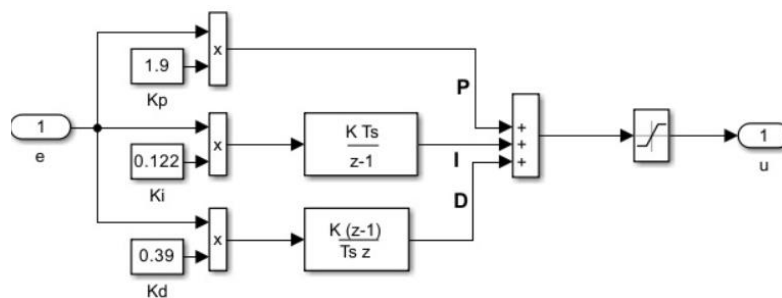


Figure 7. Discrete time PID simulation block

The PID was used as the controller in the inverted pendulum system created using the simulation model. It produces the control signal that must be applied to the cart to produce a that will maintain the angle of the inverted pendulum, θ , balanced at the intended reference value, 0° . The PID parameters were determined, as shown in Table 3 by running the simulation model using the PSO algorithm.

Table 3. PID parameters

Model Parameters	Value
K_p	85.23
K_i	150.623
K_d	0.685

Results and Discussion

Experimental control of the inverted pendulum system was performed using both the simulation model and the real system. The PID controller was used as the controller for the inverted pendulum to operate in balance. An example of the results obtained using the simulation model is shown in Figures 8 and 9. Here, by applying instantaneous force as a disturbance effect, the equilibrium position of the system is disrupted and the system is asked to come to equilibrium quickly. Similarly, an example taken from experimental studies conducted in a real system is given in Figures 10 and 11. In the real system, the equilibrium position of the pendulum was manually disturbed from outside the system, and the pendulum was asked to quickly come to balance. In Figures 9 and 11, where the equilibrium position of the simulation and real system is given, the time for the inverted pendulum to reach equilibrium is very fast and the PID keeps the system in balance.

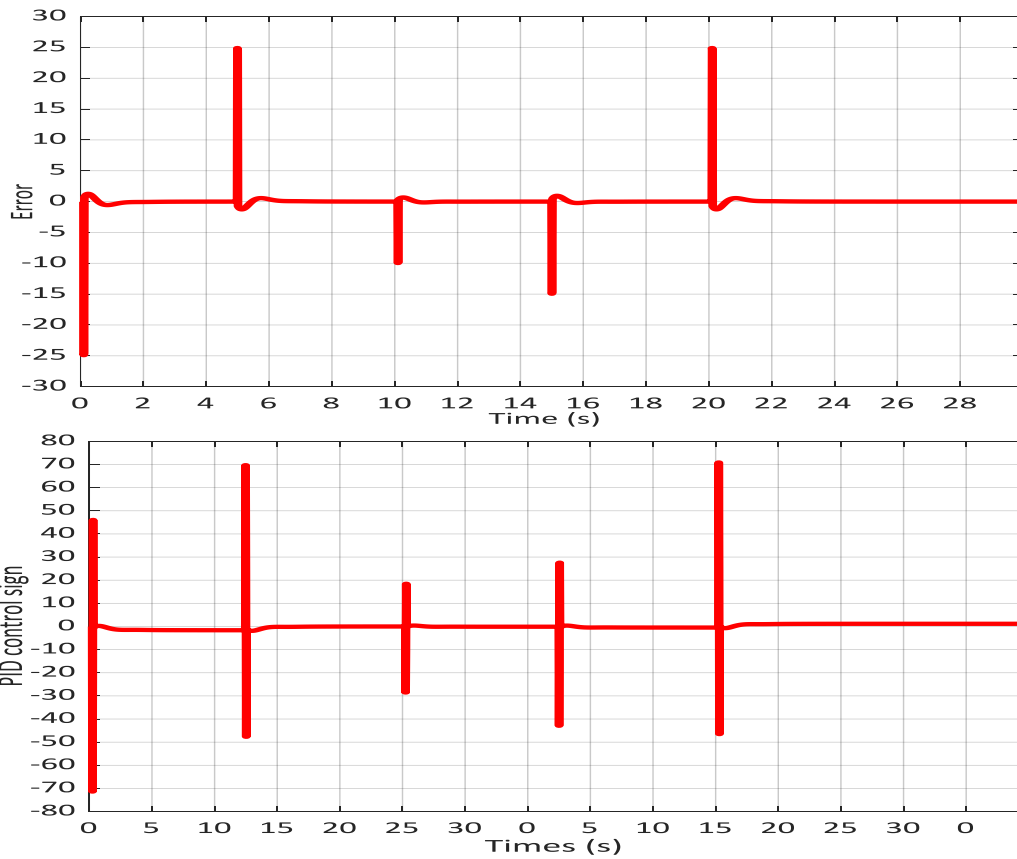


Figure 8. Simulation output of the control force produced by the PID against the error between the angle of the inverted pendulum and the reference angle.

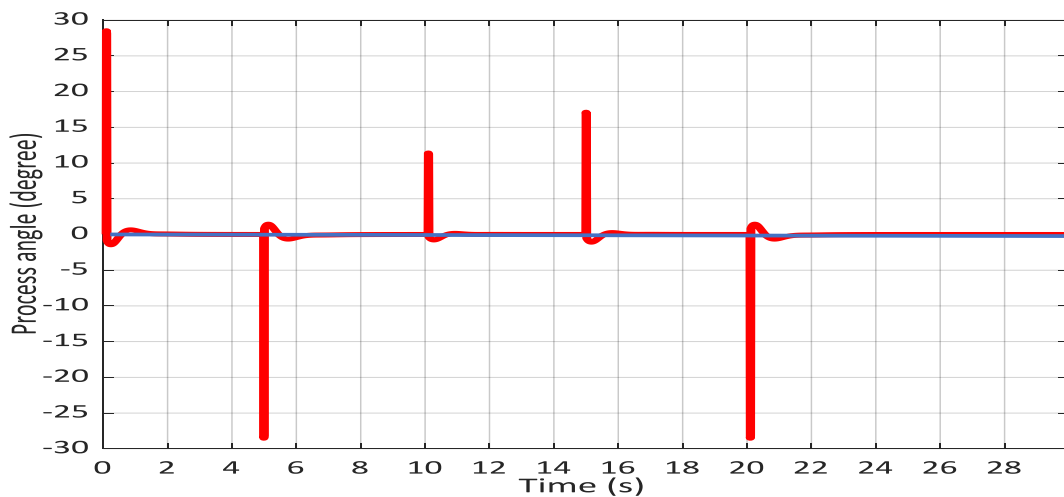


Figure 9. Simulation system angle of changes. (Red is the real system output, Blue is the reference angle.)

In Figure 9, when the PID is between 30° and 30° , it tries to keep the pendulum in balance, but when it exceeds this angle limit, because there is not enough path in the real system to bring the system back into balance, the motor is stopped and the rod falls. This decrease is shown as 0 in the graph in Figure 10.

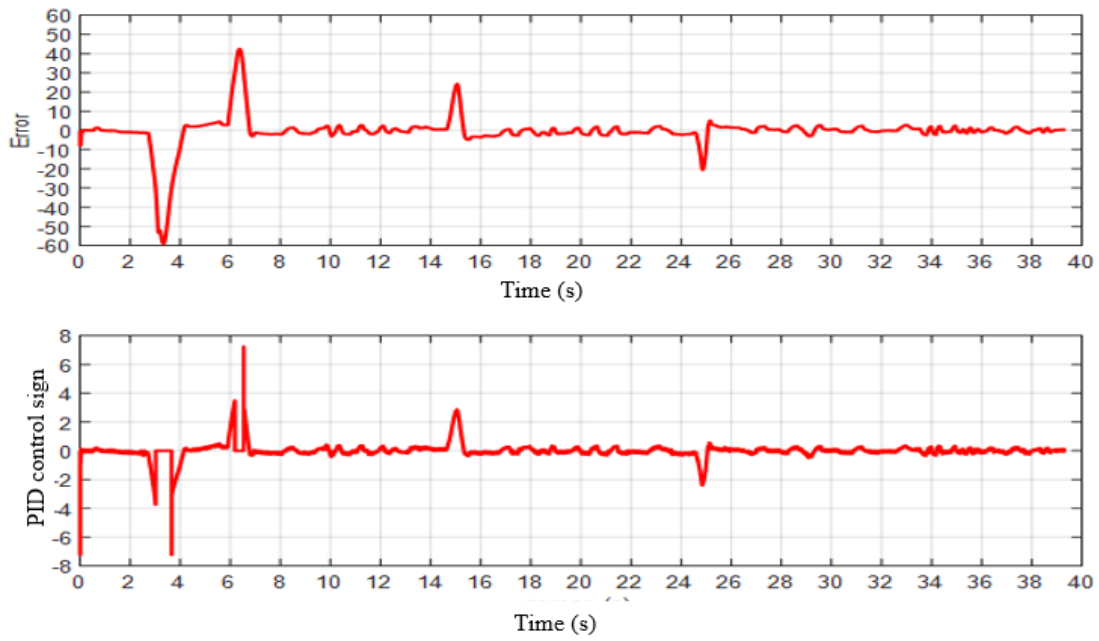


Figure 10. Control force produced by the PID against the error between the angle of the inverted pendulum and the reference angle.

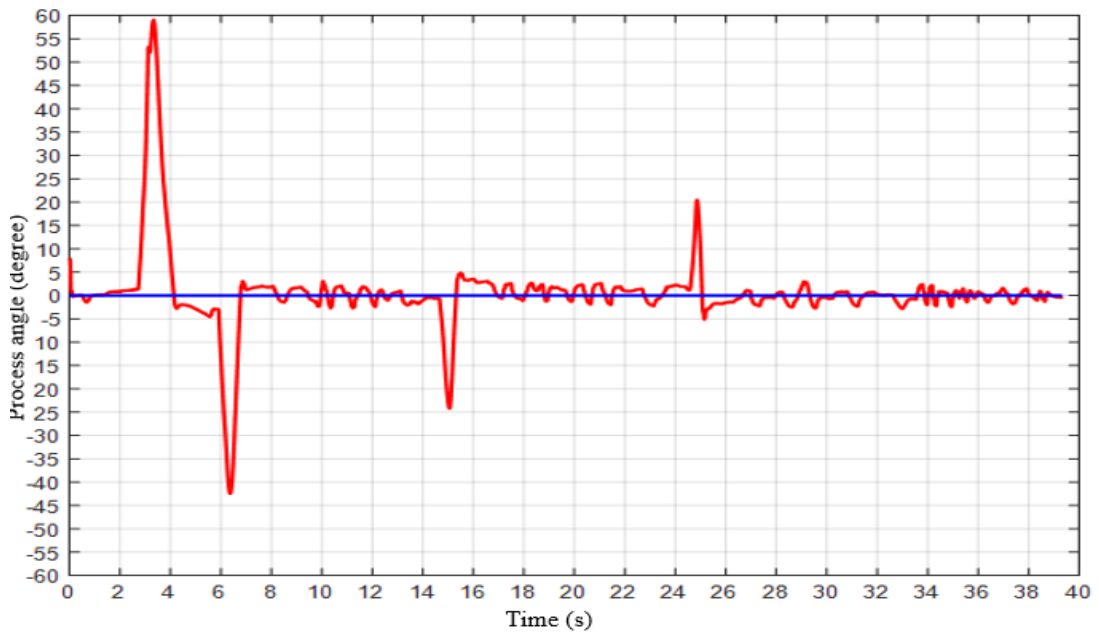


Figure 11. Real system angle of changes (Red is the real system output, Blue is the reference angle.)

Conclusion

It is difficult to find the unknown/unmeasurable parameters of in system and the control parameters of the system by experimenting on the real system. The aim of this study is to first find the unknown parameters of the system by creating a mathematical model of the system in a simulation environment, and then to obtain the PID control parameters in the simulation environment with the found parameters. Thus, to see the conformity of the control of the real system to the mathematical model and to show that the unknown parameters can be easily found through simulation.

In this study, the balance position control of the nonlinear inverted pendulum system was programed with a PID controller, PLC, which is widely used in industrial control. To control the position of the inverted pendulum system in balance, a mathematical model of the system was created, a simulation model was created, and experiments were conducted. Experiments were then conducted on a real system using the parameters obtained from the system simulation model.

In these experiments, the PID was designed as a controller to maintain the inverted pendulum in balance (vertical, 0 degrees). The PID parameters were obtained using particle swarm optimization in the simulation model. The PID parameters obtained using PSO were run as the parameters of the PID controller in the real experimental system. The simulation model shown in Figure 8 and the real experimental system shown in Figure 10 are similar. The parameters used to control the balance angle of the inverted pendulum and obtained using the simulation and optimization algorithm give similar results. It can be seen that the time required for the controller designed here to reach equilibrium is within a few seconds. In addition, fluctuations and spikes are low and the convergence speed is high. In addition, in this study, it was observed that it was easier to find the necessary parameters and design the controller by running optimization algorithms using the simulation model.

References

- [1] Mahmood Z.S. (2012). Nicelimli Kontrol Giriş i ile Ters Sarkaç Yukarı Kaldırma Benzetimi. Eskişehir Osmangazi Üniversitesi, Türkiye.
- [2] Antman S.S. (1998). The simple pendulum is not so simple. SIAM review. 40(4): 927-930.
- [3] Nasir A. N. K., Ismail R. M. T. R., Ahmad M. A. (2010). Performance Comparison Between Sliding Mode Control (SMC) and PD-PID Controllers for a Nonlinear Inverted Pendulum System. International Journal of Computer, Electrical, Automation, Control and Information Engineering. 4(10): 1508–1513.
- [4] Kizir S. (2008). Doğrusal Olmayan Ters Sarkaç Sisteminin Tasarımı ve Kontrolü. Kocaeli Üniversitesi, Türkiye.
- [5] Åström, K. J., Hägglund, T. (2006). Advanced PID control (Vol. 461). ISA-The Instrumentation, Systems, and Automation Society Research Triangle.
- [6] Acosta J. A., Gordillo F., Aracil J. (2001) Swinging up the Furuta Pendulum by the Speed Gradient Method, European Control Conference (ECC), Porto, Portugal.
- [7] Gürbüz Y., Terzioğlu R., Deniz A. (2021) Rezistif Süperiletken Arıza Akım Sınırlayıcılarının MATLAB/SIMULINK'te Modellenmesi. Avrupa Bilim ve Teknoloji Dergisi. 1(23): 173-180.
- [8] Topçu E., Bali E. (2021). DGM tekniği ile sürülen aç-kapa tipi solenoid yapıllı elektro-pnömatik fren valfinin modellenmesi ve analizi, Gazi Üniversitesi Mühendislik Mimarlık Fakültesi Dergisi. 36(3): 1417-1430.
- [9] Endiz M., Akkaya R. (2021). Matlab/Simulink ile Bipolar ve Unipolar PWM Kontrol Tekniklerinin Karşılaştırmalı Olarak İncelenmesi, Avrupa Bilim ve Teknoloji Dergisi. 1(24): 309-313.
- [10] Wei H., Wang J., Jian M., Mei S., Huang M. (2021). Steer-by-Wire Control System Based on Carsim and Simulink, 2021 IEEE International IOT Electronics and Mechatronics Conference (IEMTRONICS), DOI: 10.1109/IEMTRONICS52119.2021.9422502.
- [11] Fedullo T., Tramarin F., Vitturi S. (2020). The Impact of Rate Adaptation Algorithms on Wi-Fi-Based

Factory Automation Systems, Sensors. 20(18):5195 DOI: 10.3390/s20185195.

- [12] De las Morenas J., Da Silva C., Funchal M., Melo G. S., Vallim V. M., Leitao P. (2020). Security Experiences in IoT based applications for Building and Factory Automation, *2020 IEEE International Conference on Industrial Technology (ICIT)*, Buenos Aires, Arjantin.
- [13] Zucker G., Ferhatbegovic T., Bruckner D. (2012). Building automation for increased energy efficiency in buildings, *2012 IEEE International Symposium on Industrial Electronics*, Hangzhou, China, 28-31.
- [14] Guo B., Zhuang Z., Pan J. S., Chu S. C. (2021). Optimal design and simulation for PID controller using Fractional-Order Fish Migration Optimization algorithm, *IEEE Access*. 9(1): 8808-8819.
- [15] Noordin A., Basri M. A. M., Mohamed Z., Lazim I. M. (2021) Adaptive PID controller using sliding mode control approaches for quadrotor UAV attitude and position stabilization, *Arabian Journal for Science and Engineering*, 46(1): 963-981.
- [16] Yang B., Wang J., Wang J., Shu H., Li D., Zeng C., Yu T. (2020) Robust fractional-order PID control of supercapacitor energy storage systems for distribution network applications: A perturbation compensation-based approach, *Journal of Cleaner Production*, DOI: 10.1016/j.jclepro.2020.123362.
- [17] Acharya D., Das D. K. (2021). Swarm optimization approach to design PID controller for artificially ventilated human respiratory system, *Computer Methods and Programs in Biomedicine*, DOI: 10.1016/j.cmpb.2020.105776.
- [18] Taşkıran Z. G. Ç., Sedef H., Anday F. (2021). A new PID controller circuit design using CFOAs, *Circuits Systems and Signal Processing*, 40, 1166-1182.
- [19] Ekinci S., Hekimoğlu B., Izci D. (2021). Opposition based Henry gas solubility optimization as a novel algorithm for PID control of DC motor, *Engineering Science and Technology an International Journal*, 24(2), 331-342.
- [20] Chang, W.-D., & Shih, S.-P. (2010). PID controller design of nonlinear systems using an improved particle swarm optimization approach. *Communications in Nonlinear Science and Numerical Simulation*, 15(11), 3632–3639.
- [21] R. C. Eberhart and J. Kennedy, (1995). "A New Optimizer Using Particle Swarm Theory," in *Symposium on Micro Machine and Human Science*. Japan: Nagoya, Piscataway, NJ.